

See discussions, stats, and author profiles for this publication at: <http://www.researchgate.net/publication/254241285>

# Size Effect of Elastic and Electromechanical Properties of BaTiO<sub>3</sub> Films from First-Principles Method

ARTICLE *in* INTEGRATED FERROELECTRICS · JANUARY 2011

Impact Factor: 0.36 · DOI: 10.1080/10584587.2011.573723

---

CITATIONS

2

---

READS

76

## 3 AUTHORS:



Feng Hao

Tsinghua University

17 PUBLICATIONS 156 CITATIONS

SEE PROFILE



Jiawang Hong

Oak Ridge National Laboratory

27 PUBLICATIONS 579 CITATIONS

SEE PROFILE



Daining Fang

Tsinghua University

160 PUBLICATIONS 1,303 CITATIONS

SEE PROFILE

# Size Effect of Elastic and Electromechanical Properties of BaTiO<sub>3</sub> Films from First-Principles Method

FENG HAO,<sup>1,\*</sup> JIAWANG HONG,<sup>1</sup> AND DAINING FANG<sup>1,2</sup>

<sup>1</sup>AML, Department of Engineering Mechanics, Tsinghua University, Beijing 100084, People's Republic of China

<sup>2</sup>LTCS, College of Engineering, Peking University, Beijing 100871, People's Republic of China

*The elastic stiffness ( $C_{11}$ ) and piezoelectric coefficient ( $e_{11}$ ) of BaTiO<sub>3</sub> thin films are investigated based on first-principles calculations. It is found that the compressive stiffness of BaTiO<sub>3</sub> film is larger than its tensile stiffness. The elastic and piezoelectric properties of films are both size dependence: elastic stiffness is enhanced with decreasing film thickness, while the piezoelectricity is weakened.*

**Keywords** ferroelectric films; first-principles; elastic stiffness; size effect

## 1. Introduction

Ferroelectric thin films are of technological importance due to their ability to sustain a macroscopic polarization that can be switched by the action of an electric field. Because of the demand for smaller industrial components and the mature technology of ferroelectric thin films integrated into semiconductor chips, there is a wide application of ferroelectric thin films, such as ferroelectric memories, ferroelectric smart IC cards and ferroelectric field-effect transistors etc., covering the field of microelectronics and micro-electromechanical systems [1, 2].

Physical properties of the thin films are different from those of the corresponding bulk form. It has been observed that certain desirable bulk properties can be degraded in thin films, and some novel interesting behaviors have obtained only in thin-film form [3]. Some factors contribute to these differences, for example, the misfit strain imposed by the substrate upon which the film grows, and the thickness of ferroelectric film, etc. Epitaxial strain is one of the major factors affecting the behavior of ferroelectric thin films, which results from the mismatch of in-plane lattice parameters between ferroelectric thin films and substrate [4–6]. In the Landau-Ginsburg-Devonshire (LGD) model and phase field model, this effect is expressed by the elastic energy which depends on the elastic stiffnesses of films. However, the elastic stiffnesses of films are used as same as those of bulk [4, 7, 8]. The elastic properties of ferroelectric films are rarely reported.

Size effect is another factor that strongly influences the properties of ferroelectric nanostructures, and the critical thickness of ferroelectric films becomes an actively issue

---

Received June 2, 2010; in final form October 27, 2010.

\*Corresponding author. E-mail: haofengokli@126.com

these years. Zembilogotov *et al.* have predicted remanent polarization as a function of BaTiO<sub>3</sub> film thickness by using the mean-field Landau–Ginzburg theory [9]. Junquera *et al.* reported first principles calculations on a realistic ferroelectric–electrode interface systems, BaTiO<sub>3</sub> thin films between two metallic SrRuO<sub>3</sub> electrodes in short circuit lose their ferroelectric properties below a critical thickness of about six unit cells [10]. Kim *et al.* fabricated fully strained SrRuO<sub>3</sub>/BTO/SrRuO<sub>3</sub> heterostructures on SrTiO<sub>3</sub> substrates by pulsed laser deposition, observing polarization versus electric-field hysteresis loops, which demonstrated the existence of ferroelectricity in BTO layers with the thickness larger than 5 nm [11].

To our knowledge, the elastic properties of ferroelectric films are rarely reported, especially for the size effect of their elastic stiffnesses which has significant effect on the properties of ultrathin films. In this paper, we investigated the elastic and electromechanical properties of BaTiO<sub>3</sub> films from first-principles calculations. We demonstrated that elastic stiffnesses of BaTiO<sub>3</sub> films differ significantly under tensile strain and compressive strain. It was also found that elastic constants and piezoelectric strain coefficients are both size dependence.

## 2. Method of Calculations

Our calculations have been performed within density functional theory (DFT) and the generalized gradient approximation (GGA) [12]. We used the SIESTA method [13], based on finite-range numerical atomic orbitals, using a double- $\zeta$  polarized basis set [14]. Technical details are similar to those of Refs [15, 16]. The polarization was calculated using the geometric Berry phase approach [17]. The performance of the method was tested for bulk BaTiO<sub>3</sub>, as shown in Table 1. From the this table, it can be seen that the obtained lattice parameter for the rhombohedral phase is 0.12% smaller than the experimental value at 15 K, and 0.055% smaller than the previous results with the same GGA and plane waves as basis set [12]. The rhombohedral angle is 89.84° which is the same as obtained in the experiment. The spontaneous polarization has been tested in Ref [18], in which our result is 0.43C/m<sup>2</sup>

**Table 1**

Structural parameters for rhombohedral  $R3m$  BaTiO<sub>3</sub> bulk, the atom positions  $u_z$  are given in terms of the lattice constants.

	LSD <sup>a</sup>	PBE <sup>a</sup>	WC <sup>a</sup>	This work	Expt(15 K) <sup>b</sup>
$a$ (Å)	3.9492	4.0713	4.0009	3.9987	4.0036
$\alpha$	89.91°	89.65°	89.86°	89.84°	89.84°
Vol (Å <sup>3</sup> )	61.59	67.47	64.04	63.94	64.17
$u_z$ (Ba)	0.00	0.00	0.00	0.00	0.00
$u_z$ (Ti)	0.4901	0.4845	0.4883	0.4875	0.4870
$u_z$ (O <sub>1</sub> O <sub>2</sub> )	0.5092	0.5172	0.5116	0.5117	0.5109
$u_z$ (O <sub>3</sub> )	0.0150	0.0295	0.0184	0.0172	0.0193

Exchange-correlation functionals: LSD–local spin density; PBE: Perdew-Burke-Ernzerhof functional; WC: Wu-Cohen modification of PBE functional.

<sup>a</sup>See reference 12.

<sup>b</sup>See reference 23.

along [111], very close to previous theoretical results  $0.44\text{C}/\text{m}^2$  [19] (the experimental result is  $0.35\text{C}/\text{m}^2$  [20]).

We focused on stoichiometric BaTiO<sub>3</sub> thin films, with one face terminated with BaO and the other face terminated with TiO<sub>2</sub>. The  $z$  axis was taken as normal to the surface, while the  $x$  and  $y$  axes were in-plane. The film thickness was specified by an integer  $n$  that corresponds to the number of unit cells along the  $z$  direction (out of plane). Integrals in reciprocal space used a  $\bar{k}$  mesh of  $10\text{ \AA}$  cutoff [21] while the integrals in real space used a  $\bar{r}$  mesh of  $350\text{ Ry}$  cutoff [22]. The atomic positions were relaxed until all atomic force components were smaller than  $10\text{ meV}/\text{\AA}$ . Periodic replicas of the films were separated by  $16\text{ \AA}$  of vacuum.

For the mechanical properties of BaTiO<sub>3</sub> films, we focused on the elastic constants of films. The theoretical elastic constants were calculated from the energy variation by imposing small strains to the equilibrium unit cell. The elastic energy under strain was given by

$$\Delta E = \frac{V}{2} \sum_{i=1}^6 \sum_{j=1}^6 C_{ij} \varepsilon_i \varepsilon_j \quad (1)$$

Where  $V$  is the volume of the initial unit cell undistorted,  $\Delta E$  is the energy increment between  $E$  (the unit cell energy under the strain) and  $E_0$  (the unit cell energy without the strain) under the strain  $\varepsilon = (\varepsilon_1, \varepsilon_2, \varepsilon_3, \varepsilon_4, \varepsilon_5, \varepsilon_6)$ , and  $C_{ij}$  is the second-rank tensor related to stress and strain.

For the tetragonal crystal system of single-crystal BaTiO<sub>3</sub>, the elastic stiffness tensor  $C$  is written by

$$C = \begin{pmatrix} c_{11} & c_{12} & c_{13} & 0 & 0 & 0 \\ c_{21} & c_{22} & c_{23} & 0 & 0 & 0 \\ c_{31} & c_{32} & c_{33} & 0 & 0 & 0 \\ 0 & 0 & 0 & c_{44} & 0 & 0 \\ 0 & 0 & 0 & 0 & c_{55} & 0 \\ 0 & 0 & 0 & 0 & 0 & c_{66} \end{pmatrix} \quad (2)$$

where  $c_{11} = c_{22}$ ,  $c_{12} = c_{21} = c_{13} = c_{31}$ ,  $c_{44} = c_{55}$ , and  $c_{66} = (c_{11} - c_{12})/2$ . Thus there are only five independent component in stiffness tensor, which can be conveniently calculated out by applying strain  $\varepsilon$  on a initial unit cell with following models [24]:

Mode 1:  $\varepsilon = (\delta, 0, 0, 0, 0, 0)$

$$\frac{\Delta E}{V} = \frac{1}{2} C_{11} \delta^2 \quad (3)$$

Mode 2:  $\varepsilon = (\delta, \delta, 0, 0, 0, 0)$

$$\frac{\Delta E}{V} = (C_{11} + C_{12}) \delta^2 \quad (4)$$

Mode 3:  $\varepsilon = (0, 0, \delta, 0, 0, 0)$

$$\frac{\Delta E}{V} = \frac{1}{2} C_{33} \delta^2 \quad (5)$$

**Table 2**  
Elastic stiffnesses for BaTiO<sub>3</sub> bulk material

Elastic Stiffness (GPa)	C <sub>11</sub>	C <sub>12</sub>	C <sub>33</sub>	C <sub>66</sub>
This paper	194	125	154	130
Experiment <sup>a</sup>	211	107	160	127
<i>ab initio</i> <sup>b</sup>	282 ~ 352	107 ~ 135	/	/

<sup>a</sup>See reference 25.

<sup>b</sup>See reference 26.

Mode 4:  $\varepsilon = (0, 0, 0, 0, 0, \delta)$

$$\frac{\Delta E}{V} = \frac{1}{2} C_{66} \delta^2 \quad (6)$$

In order to apply proper strain, we change the lattice constant and fix it during the relaxation. For instance, in order to apply strain  $\varepsilon$  to the equilibrium system with lattice constant  $a$  in case of Model 1, the lattice constant along  $x$  direction is changed to  $(1 + \delta)a$  and fixed during the relaxation.

We can change the lattice constant to apply the proper strain. For instance, in order to apply strain  $\varepsilon$  for a equilibrium system with lattice constant  $a$ , we can change the lattice constant to  $(1 + \varepsilon)a$  and fix it during the relaxation.

Using this method, we calculated the elastic stiffnesses for BaTiO<sub>3</sub> bulk, compared with experimental data [25] and previous *ab initio* results [26], as shown in Table 2. It can be seen from this table that our results are consistent with the experimental results.

Piezoelectricity is a phenomenon incorporating the electromechanical effects, for instance, mechanical stress can lead to an induced electric polarization whose magnitude is proportional to the applied stress, and it can be mathematically defined by:

$$P_i = d_{ij} \sigma_j \quad (7)$$

where  $P_i$  is the stress-induced polarization,  $\sigma_j$  is stress tensor and  $d_{ij}$  is a third-rank piezoelectric stress tensor,  $i = 1, 2, 3$  and  $j = 1, 2, 3, 4, 5, 6$ , using the Voigt notation and the Einstein summation convention.

There also exist another piezoelectric equations linking polarization and strain.

$$P_i = e_{ij} \varepsilon_j \quad (8)$$

Where  $P_i$  is the strain-induced polarization,  $\varepsilon_j$  is strain tensor, and the  $e_{ij}$  is piezoelectric strain coefficients which is also a third-rank tensor.

We used Eq. (8) to calculate the piezoelectric strain coefficients  $e_{ij}$ . Piezoelectric stress coefficient  $d_{ij}$  would be easily obtained after  $e_{ij}$  calculated because they are related to each other by the elastic stiffnesses or elastic compliances [27].

### 3. Results and Discussions

We calculated BaTiO<sub>3</sub> films with  $n = 2$  to 5. Table 3 shows our results of the in-plane lattice constant of films. It shows that the in-plane lattice constants increase with increment of film thickness and constant of film ( $n = 5$ ) is very close to that of bulk (0.3999 nm).

**Table 3**  
The in-plane lattice constant for films

Cell Number	$n = 2$	$n = 3$	$n = 4$	$n = 5$
Lattice Constant (nm)	0.3945	0.3968	0.3981	0.3989

The elastic constant  $C_{11}$  were calculated according to the Eq. (3), for the films of  $n = 2$  to 5. It is found that the position of the minimum energy state deviates from the position of  $\varepsilon_{11} = 0$  if the data under tensile and compressive strain are fitted together according to Eq. (3). The reason is that BaTiO<sub>3</sub> is brittle material and its tensile stiffness  $C_{11}^T$  is inconsistent with compressive stiffness  $C_{11}^C$ . Therefore,  $C_{11}^T$  and  $C_{11}^C$  were fitted separately. Figure 1 shows this fitting for film of  $n = 2$ .

Figure 2(a) shows the size effect of elastic stiffness  $C_{11}$  under tensile and compressive strain for different films. From this figure we can see that the tensile stiffness is smaller than compressive stiffness for a film, but they are both size dependant. The elastic stiffness  $C_{11}$  of BaTiO<sub>3</sub> film reduces as film thickness increases. It should be noted that the compressive stiffness is very close to that of BaTiO<sub>3</sub> bulk when the thickness reaches  $n = 5$ , i.e.  $\sim 2.0$  nm.

We also calculated the polarization of films and found that the out-of-plane polarization is zero for films of  $n = 2$  to 5. However, the in-plane polarizations along [110] are nonzero and they increase as the thickness becomes larger, as shown in Fig. 2(b). This also indicates that the BaTiO<sub>3</sub> thin films are not tetragonal structures after relaxation.

Piezoelectric strain coefficients were calculated for BaTiO<sub>3</sub> bulk and films of  $n = 2$  and 4. For tetragonal BaTiO<sub>3</sub> bulk, tensile strains of  $\varepsilon_{33} = -0.5\%$ ,  $-1\%$ ,  $-1.5\%$ ,  $-2\%$  along [001] were applied and the piezoelectric strain coefficient  $e_{33}$  was obtained

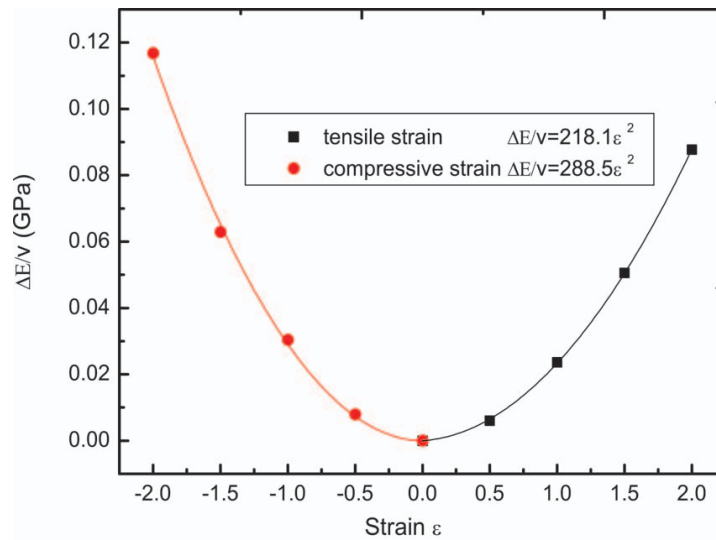


**Figure 1.** Elastic stiffness  $C_{11}$  under tensile strain and compressive strain for BaTiO<sub>3</sub> film ( $n = 2$ ).

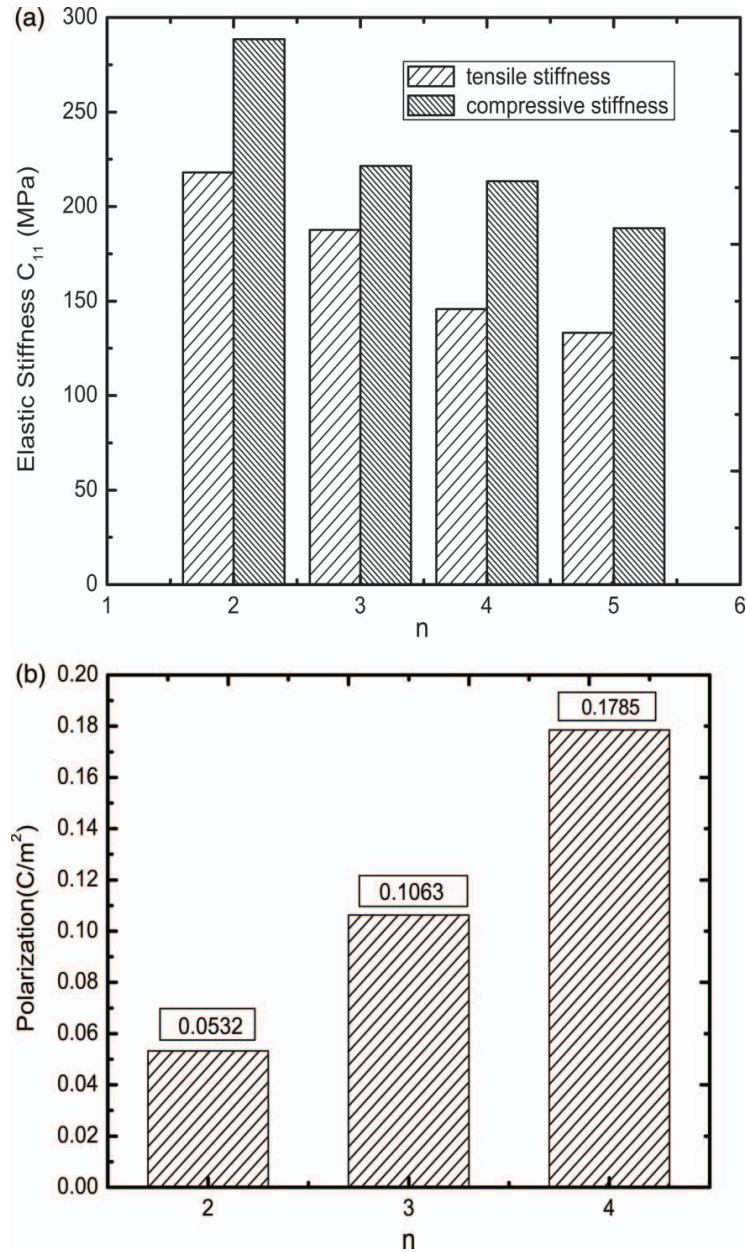


**Figure 2.** (a) Size effect of elastic stiffness  $C_{11}$  for BaTiO<sub>3</sub> films under tensile and compressive strain; (b) size effect of in-plane polarization along (110) direction.

after calculating the polarization under different strain. For films, the tensile strains of  $\varepsilon_{11} = -0.5\%$ ,  $-1\%$ ,  $-1.5\%$ ,  $-2\%$  were applied along [100] and  $e_{11}$  was obtained. The results are shown in Fig. 3. For the bulk,  $e_{33}$  is  $17.9 \text{ C/m}^2$ , which agrees with previous result of  $18.6 \text{ C/m}^2$  in Ref [28]. The piezoelectric properties of BaTiO<sub>3</sub> films show size dependence:  $e_{11}$  decreases with reduction of film thickness.

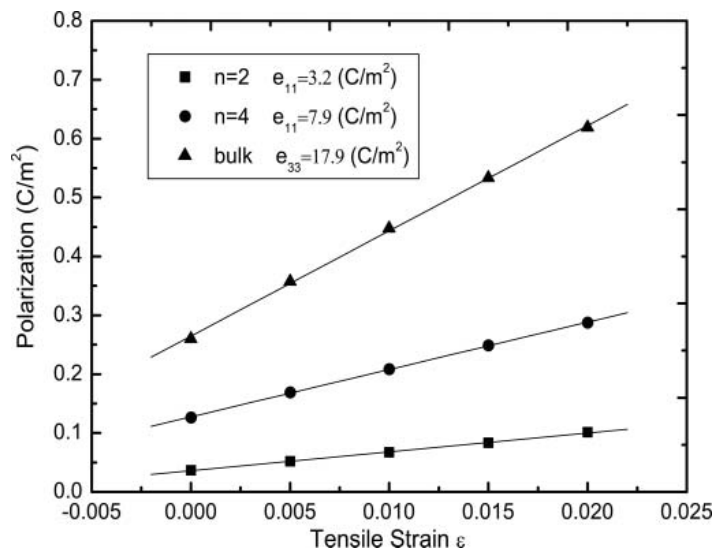


**Figure 3.** The piezoelectric properties for BaTiO<sub>3</sub> bulk and thin films,  $e_{33}$  for bulk and  $e_{11}$  for films of  $n = 2$  and  $n = 4$ .

#### 4. Conclusion

In summary, the elastic and electromechanical properties of BaTiO<sub>3</sub> thin films were explored from first-principles calculations. By fitting the energy-strain diagram, it was found the inconsistency of elastic properties under tensile and compressive strain: the compressive stiffness is significantly greater than the tensile stiffness. In addition, the elastic stiffness  $C_{11}$  decreases as the film thickness increases, on the contrary, the piezoelectric strain coefficient increases with the increasing of the film thickness.

#### References

1. J. F. Scott and C. A. P. Dearaujo, Ferroelectric Memories. *Science*. **246**, 1400–1405 (1989).
2. J. F. Scott, Applications of Modern Ferroelectrics. *Science*. **315**, 954–959 (2007).
3. M. Dawber, K. M. Rabe, and J. F. Scott, Physics of thin-film ferroelectric oxides. *Rev. Mod. Phys.* **77**, 1083–1130 (2005).
4. N. A. Pertsev, A. G. Zembilgotov, and A. K. Tagantsev, Effect of mechanical boundary conditions on phase diagrams of epitaxial Ferroelectric Thin Films. *Phys. Rev. Lett.* **80**, 1988–1991 (1998).
5. K. J. Choi, M. Biegalski, and Y. L. Li, Enhancement of ferroelectricity in strained BaTiO<sub>3</sub> thin film. *Science*. **306**, 1005–1009 (2004).
6. C. Ederer and N. A. Spaldin, Effect of epitaxial strain on the spontaneous polarization of thin film ferroelectrics. *Phys. Rev. Lett.* **95**, 25761 (2005).
7. Y. L. Li, S. Y. Hu, Z. K. Liu, and L. Q. Chen, Phase-field model of domain structures in ferroelectric thin films. *Appl. Phys. Lett.* **78**, 3878–3880 (2001).
8. Y. H. Zhang, J. Y. Li, and D. N. Fang, Size dependent domain configuration and electric field driven evolution in ultrathin ferroelectric films: A phase field investigation. *J. Appl. Phys.* **107**, 034107 (2010).
9. A. G. Zembilgotov, N. A. Pertsev, H. Kohlstedt, and R. Waser, Ultrathin epitaxial ferroelectric films grown on compressive substrates: Competition between the surface and strain effects. *J. Appl. Phys.* **91**, 2247 (2002).

10. J. Junquera and P. Ghosez, Critical thickness for ferroelectricity in perovskite ultrathin films. *Nature*. **422**, 506–509 (2003).
11. Y. S. Kim, D. H. Kim, and J. D. Kim, Critical thickness of ultrathin ferroelectric BaTiO<sub>3</sub> films. *Appl. Phys. Lett.* **86**, 102907 (2005).
12. Z. Wu and R. E. Cohen, More accurate generalized gradient approximation for solids. *Phys. Rev. B*. **73**, 235116 (2006).
13. J. M. Soler, E. Artacho, J. D. Gale, A. Garcia, J. Junquera, P. Ordejon, and D. S. Portal, The SIESTA method for ab initio order-N materials simulation. *J. Phys. Condens. Matter*. **14**, 2745–2779 (2002).
14. E. Anglada, J. M. Soler, J. Junquera, and E. Artacho, Systematic generation of finite-range atomic basis sets for linear-scaling calculations. *Phys. Rev. B*. **66**, 205101 (2002).
15. J. W. Hong, G. Catalan, J. F. Scott, and E. Artacho, The flexoelectricity of barium and strontium titanates from first principles. *J. Phys. Condens Matter*. **22**, 112201 (2010).
16. J. W. Hong, G. Catalan, D. N. Fang, E. Artacho, and J. F. Scott, Topology of the polarization field in ferroelectric nanowires from first principles. *Phys. Rev. B*. **81**, 172101 (2010).
17. R. D. King-Smith and D. Vanderbilt, Theory of polarization of crystalline solids. *Phys. Rev. B*. **47**, 1651–1654 (1993).
18. Y. H. Zhang, J. W. Hong, B. Liu, and D. N. Fang, Molecular dynamics investigations on the size-dependent ferroelectric behavior of BaTiO<sub>3</sub> nanowires. *Nanotechnology*. **20**, 405703 (2009).
19. W. Zhong, R. D. King-Smith, and D. Vanderbilt, Giant LO-TO splittings in perovskite ferroelectrics. *Phys. Rev. Lett.* **72**, 3618–3621 (1994).
20. H. Wieder, Electrical behavior of barium titanate single crystals at low temperatures. *Phys. Rev.* **99**, 1161–1165 (1955).
21. J. Moreno and J. M. Soler, Optimal meshes for integrals in real-space and reciprocal-space unit cells. *Phys. Rev. B*. **45**, 13891–13898 (1992).
22. J. M. Soler, E. Artacho, J. D. Gale, A. Garcia, J. Junquera, P. Ordejon, and D. S. Portal, The SIESTA method for ab initio order-N materials simulation. *J. Phys. Condens Matter*. **14**, 2745–2779 (2002).
23. G. H. Kwei, A. C. Lawson, S. J. L. Billinge, and S. W. Cheong, Structures of the ferroelectric phases of barium titanate. *J. Phys. Chem.* **97**, 2368–2377 (1993).
24. S. Q. Wang and H. Q. Ye, First-principles study on elastic properties and phase stability of III-V compounds. *Phys Stat Sol.* **240**, 45–54 (2003).
25. Z. Li, S. K. Chan, M. H. Grimsditch, and E. S. Zouboulis, The elastic and electromechanical properties of tetragonal BaTiO<sub>3</sub> single crystals. *J Appl Phys.* **70**, 7327–7332 (1991).
26. S. Piskunov, E. Heifets, R. I. Eglitis, and G. Borstel, Bulk properties and electronic structure of SrTiO<sub>3</sub>, BaTiO<sub>3</sub>, PbTiO<sub>3</sub> perovskites: an ab initio HF/DFT study. *Computational Materials Science*. **29**, 165–178 (2004).
27. L. Bellaiche, Piezoelectricity of ferroelectric perovskites from first principles. *Curr. Opin. Solid State Mater. Sci.* **6**, 19–25 (2002).
28. F. Ramirez, P. R. Heyliger, and E. Pan, Discrete layer solution to free vibrations of functionally graded magneto-electro-elastic plates. *Mech. Adv. Mater. Struc.* **13**, 249–266 (2006).